The $a^1\Delta_g \rightarrow X^3\Sigma_g^-$ Transition in Molecular Oxygen: Interpretation of Solvent Effects on Spectral Shifts

Tina D. Poulsen and Peter R. Ogilby*

Department of Chemistry, Aarhus University, Langelandsgade 140, DK-8000 Århus C, Denmark

Kurt V. Mikkelsen*

Chemical Laboratorium III, Department of Chemistry, H. C. Ørsted Institute, University of Copenhagen, DK-2100 Copenhagen Ø, Denmark

Received: December 17, 1998; In Final Form: March 8, 1999

Ab initio computational methods have been used to investigate the effect of solvent on the $a^1\Delta_g \rightarrow X^3\Sigma_g^-$ transition in molecular oxygen. For a given solvent molecule, M, energies have been obtained for the $M-O_2(a^1\Delta_g)$ complex that is in equilibrium with its surrounding outer solvent and for the $M-O_2(X^3\Sigma_g^-)$ complex that is not in equilibrium with the outer solvent (i.e., the Franck−Condon state populated in the $a \rightarrow X$ transition). These energies depend principally on the quadrupolar and higher order coupling terms between the complex and the outer solvent and only minimally on the dipolar coupling term and on dispersion interactions. Upon averaging over multiple $M-O_2$ orientations, each with an unique transition probability, differences between the calculated $O_2(a^1\Delta_g)$ and $O_2(X^3\Sigma_g^-)$ energies correlate well with the experimental spectral data. Thus, previously published correlations between experimental a−X spectral shifts and the solvent polarizability cannot be ascribed solely to a dispersion interaction, but rather simply reflect the general importance of the solvent's electronic response in the oxygen−solvent interaction.

Introduction

Transitions between the three lowest electronic states of molecular oxygen are extremely sensitive to perturbations and thus yield an informative system for the study of equilibrium and nonequilibrium solvent effects. Consequently, oxygen's radiative transitions in solution continue to be a subject of great interest.[1−10]

In the gas phase, the $O_2(b^1\Sigma_g^+)-O_2(a^1\Delta_g)$, $O_2(a^1\Delta_g)-O_2(X^3\Sigma_g^-)$, and $O_2(b^1\Sigma_g^+)-O_2(X^3\Sigma_g^-)$ transitions in oxygen are forbidden as electric dipole processes.[11] In solution, solvent-dependent perturbations cause (1) the transitions to become more probable and (2) the transition energies to decrease, as reflected in emission spectra that are red-shifted relative to the gas-phase values. In this paper, we address the issue of solvent effects on the a−X spectral shift.

Interpretations of the experimental data have focused on the fact that a−X spectral shifts correlate reasonably well with either the solvent refractive index, n, or functions of n, such as $(n^2 - 1)/(n^2 + 2)$. Specifically, the difference between the solution and gas-phase emission maxima appears to increase linearly as n increases. On this basis, models have been proposed in which the spectral shift derives principally from a dispersion interaction with a solvent molecule.[6−8,12] In the most extensive study thus far,[6] the London formula was employed to calculate the a−X spectral shift, $\Delta\nu_{calc}^{a-X}$.

$$\Delta\nu_{calc}^{a-X} = -\frac{1.5\alpha_{sol}}{R_{int}^6}\left[\alpha_a\frac{IP_a IP_{sol}}{IP_a + IP_{sol}} - \alpha_X\frac{IP_X IP_{sol}}{IP_X + IP_{sol}}\right] \quad (1)$$

In this expression, R_{int} denotes the interaction distance between oxygen and the perturbing solvent molecule, α_{sol} denotes the polarizability of the solvent, α_X and α_a denote the polarizabilities of the respective states of oxygen, and IP denotes the ionization potential of the indicated species.

Despite the apparent succes of eq 1 to model the a−X experimental data,[6] we recently showed that this equation alone cannot account for the trend in the plots of $\Delta\nu$ vs functions of n and that such plots can mislead one to believe that dispersion forces are a key parameter in the oxygen−solvent interaction.[13] In the application of the London expression mentioned above,[6] it was assumed that α_a was almost twice as large as α_X. We have shown, however, that although excited-state polarizabilities are indeed often larger than that of the ground state, in fact α_a does not differ significantly from α_X.[13] Moreover, depending on both the solvent and the solvation conditions, α_a can even be *smaller* than α_X. In reaching these conclusions, we employed a model in which an isolated O_2 molecule was surrounded by the solvent which, in turn, was regarded as a homogeneous dielectric medium.

In an attempt to better understand phenomena that give rise to the solvent-dependent spectral shifts in oxygen, we set out to employ high-level, ab initio computational methods to characterize the variety of interactions possible between a solvent molecule, M, and oxygen. We first considered it important to ascertain whether our conclusions regarding α_a and α_X obtained for the isolated molecule also hold true for an $M-O_2$ complex. We then considered it necessary to employ dielectric models generalized to include nonequilibrium as well as equilibrium solvation.[14−16] Continuum and semicontinuum approaches were used. In the continuum model, we enclosed

* To whom correspondence should be addressed.

10.1021/jp984782i CCC: $18.00
Published on Web 04/17/1999

O_2 in a spherical cavity surrounded by a homogeneous dielectric medium characterized by the macroscopic static and optical dielectric constants, ϵ_{st} and ϵ_{op}. Even though the model enables a proper electrostatic description of the long-range Coulombic interactions, it neglects short-range interactions. In the semicontinuum approach, we modeled a first solvation shell by forming a complex between one oxygen molecule and one solvent molecule, M, and embedded this $M-O_2$ complex in a dielectric medium. Under these conditions, it is still possible to treat the system on a high ab initio level and include short-range interactions as well. The results of these studies are reported herein.

Methods and Computational Details

A. Geometries. In all calculations, the intramolecular geometries of the solvent molecule, M, and the oxygen molecule were fixed. Solvent molecule geometries were obtained using experimental bond lengths and angles.[17] Since we are considering the $a \rightarrow X$ transition, we employed the $O_2(a^1\Delta_g)$ bond length for the initial as well as the final Franck−Condon state. The value used, 1.23 Å, is consistent with the experimental bond length, 1.216 Å,[11] and the optimized geometry for the employed active space and basis set, 1.236 Å. However, we determined that $O_2(a^1\Delta_g)-O_2(X^3\Sigma_g^-)$ energy differences are relatively insensitive to minor changes in the oxygen bond length. In the calculations, we oriented M and O_2 in a number of different ways, and for each orientation we computed the $M-O_2$ energy at different intermolecular distances.

B. Phosphorescence Rates. Because $a \rightarrow X$ spectra obtained from experiments are most conveniently characterized by the band maximum, ν_{max}, it is desirable to likewise calculate the corresponding quantity. This can be achieved by taking a weighted average of the solvent shifts for the a−X transition calculated for a variety of $M-O_2$ orientations. Because the $M-O_2$ potential surfaces are very shallow (i.e., energy differences between one $M-O_2$ orientation and another are small, which gives similar Boltzmann factors), an appropriate weighting factor is the phosphorescence rate of the $M-O_2(a^1\Delta_g) \rightarrow M-O_2(X^3\Sigma_g^-)$ transition.

For each $M-O_2$ orientation, the phoshorescence rate was determined from quadratic response calculations generalized to include operators of singlet as well as triplet spin,[18] and the singlet−triplet transition moments were evaluated as the residues of the quadratic response functions. Although phosphorescence rates thus obtained depend on the basis set and size of active space used[18] and may not be accurate in an absolute sense, relative values of these rates for a given $M-O_2$ complex are sufficient for the generation of the desired weighting factors.

C. Solvent. The solvent molecules employed are benzene (C_6H_6), carbon disulfide (CS_2), acetonitrile (CH_3CN), carbon tetrachloride (CCl_4), and acetone ($(CH_3)_2CO$). The reason for choosing these solvents is that the molecules are small and they all contain one or more symmetry elements that simplify the calculations. Furthermore, these solvents cover a broad range of static, ϵ_{st}, and optical, $\epsilon_{op} = n^2$, dielectric constants (Tables 1 and 2).

To model the solvation of either O_2 or an $M-O_2$ complex, we regard the solvent as a homogeneous dielectric medium that surrounds a spherical cavity containing the solute. The medium is characterized by ϵ_{st} and ϵ_{op} and gives a reaction field with a self-consistent coupling to the charge distribution of the solute.

TABLE 1. Comparison between Experimental Values and Values Calculated Using the Dielectric Continuum Model for *a*−*X* Emission Spectral Shifts, $\Delta\nu$

			spectral shift (cm^{-1})		
solvent	ϵ_{st}	ϵ_{op}	aug-cc-pVDZ	aug-cc-pVQZ	expt[a]
C_6H_6	2.28	2.253	−98	−100	−42.9
CS_2	2.64	2.647	−112	−113	−53.2
CH_3CN	37.5	1.806	−393	−376	−30.9
CCl_4	2.24	2.132	−99	−102	−32.3
$(CH_3)_2CO$	20.7	1.847	−372	−356	−29.8

[a] Data from an FTIR emission study.[8] $\Delta\nu = \nu_{max}$(solution) − ν_{max}(gas).

TABLE 2. Comparison between Experimental Values and Values Calculated Using the Semicontinuum Model for *a*−*X* Emission Spectral Shifts, $\Delta\nu$

solvent	dielectric constants	$\Delta\nu_{calc}$[a] (cm^{-1})	weight factor[b]	$\Delta\nu_{calc}$ (average) (cm^{-1})	$\Delta\nu_{expt}$[c] (cm^{-1})
C_6H_6	$\epsilon_{st} = 2.28$	(a) −44.5	0.498	−39.2	−42.9
	$\epsilon_{op} = 2.253$	(b) −34.0	0.502		
CS_2	$\epsilon_{st} = 2.64$	(a) −64.3	0.109	−63.4	−53.2
	$\epsilon_{op} = 2.647$	(b) −47.7	0.306		
		(c) −71.4	0.585		
CH_3CN	$\epsilon_{st} = 37.5$	(a) −28.1	0.048	−44.4	−30.9
	$\epsilon_{op} = 1.806$	(b) −57.1	0.653		
		(c) −19.5	0.299		
CCl_4	$\epsilon_{st} = 2.24$	(a) −24.8	0.854	−26.5	−32.3
	$\epsilon_{op} = 2.132$	(b) −36.4	0.042		
		(c) −36.8	0.104		
$(CH_3)_2CO$	$\epsilon_{st} = 20.7$	(a) −47.2	0.425	−28.4	−29.8
	$\epsilon_{op} = 1.847$	(b) −14.5	0.575		

[a] Separate numbers reflect different M and O_2 orientations. The letters refer to the corresponding figures. [b] A factor that reflects the *a*−*X* transition probability for the given $M-O_2$ orientation (see text). [c] Data from an FTIR emission study.[8] $\Delta\nu = \nu_{max}$ (solution) − ν_{max} (gas).

The total polarization is the sum of two contributions:[19−31]

$$\mathbf{P}(\mathbf{r}) = \mathbf{P}_{op}(\mathbf{r}) + \mathbf{P}_{in}(\mathbf{r}) \qquad (2)$$

The optical polarization, $\mathbf{P}_{op}$, represents the response from the electronic degrees of freedom of the solvent, and $\mathbf{P}_{op}$ is assumed always to be in equilibrium with the charge distribution of the solute because of its very short relaxation time. The inertial polarization, $\mathbf{P}_{in}$, represents the response from the nuclear degrees of freedom of the solvent molecules (vibrational, rotational, and translational degress of freedom). This part of the polarization remains fixed during an electronic transition, and it is thus not always in equilibrium with the molecular charge distribution of the solute. We thus have (1) a situation where the solvent is not in equilibrium with the molecular charge distribution of the solute, and the solvent−solute interactions depend on ϵ_{op} as well as ϵ_{st}, and (2) an equilibrium situation in the limit of a static perturbation where the response of the dielectric medium is represented only by ϵ_{st}.

To apply our data to $O_2(a^1\Delta_g)$ *emission*, we consider that the initial state, $a^1\Delta_g$, is in equilibrium with the surrounding solvent whereas the final state, $X^3\Sigma_g^-$, is not. Thus, when compared to a gas-phase system, $O_2(a^1\Delta_g)$ will be stabilized more than $O_2(X^3\Sigma_g^-)$, and the solution-phase a−X transition will occur at a lower energy than the corresponding gas-phase transition. The solvent shift, $\Delta\nu$, is defined as the difference between these transition energies, $E_{sol} - E_{gas}$, and thus yields a negative number (a red shift).

The energies for the initial equilibrium state and the final nonequilibrium state are given by[19,20]

$$E_{\mathrm{i}}^{\mathrm{eq}} = \langle \mathrm{i}|H_{\mathrm{vac}}|\mathrm{i}\rangle + \sum_{\iota,\mathrm{m}} g_\iota(\epsilon_{\mathrm{st}})\langle T_{\iota\mathrm{m}}(\rho_{\mathrm{i}})\rangle^2 \quad (3)$$

$$\begin{aligned} E_{\mathrm{f}}^{\mathrm{neq}} &= \langle \mathrm{f}|H_{\mathrm{vac}}|\mathrm{f}\rangle + \sum_{\iota,\mathrm{m}} g_\iota(\epsilon_{\mathrm{op}})\langle T_{\iota\mathrm{m}}(\rho_{\mathrm{f}})\rangle^2 + \\ &\quad \sum_{\iota,\mathrm{m}} g_\iota(\epsilon_{\mathrm{st}},\epsilon_{\mathrm{op}})\langle T_{\iota\mathrm{m}}(\rho_{\mathrm{i}})\rangle[2\langle T_{\iota\mathrm{m}}(\rho_{\mathrm{f}})\rangle - \langle T_{\iota\mathrm{m}}(\rho_{\mathrm{i}})\rangle] \\ &= \langle \mathrm{f}|H_{\mathrm{vac}}|\mathrm{f}\rangle + \sum_{\iota,\mathrm{m}} g_\iota(\epsilon_{\mathrm{st}})\langle T_{\iota\mathrm{m}}(\rho_{\mathrm{f}})\rangle^2 - \\ &\quad \sum_{\iota,\mathrm{m}} g_\iota(\epsilon_{\mathrm{st}},\epsilon_{\mathrm{op}})[\langle T_{\iota\mathrm{m}}(\rho_{\mathrm{i}})\rangle - \langle T_{\iota\mathrm{m}}(\rho_{\mathrm{f}})\rangle]^2 \quad (4) \end{aligned}$$

where ρ_{i} and ρ_{f} are the molecular charge distributions of the initial and final states of the solute, respectively, and $\langle T_{\iota\mathrm{m}}(\rho)\rangle$ are the charge moments. The maximum ι value is equal to 10.

The reaction field factors, g_ι, are given by[19]

$$g_\iota(\epsilon) = -\frac{1}{2} r_{\mathrm{c}}^{-(2\iota+1)} \frac{(\iota+1)(\epsilon-1)}{[\iota+\epsilon(\iota+1)]} \quad (5)$$

$$g_\iota(\epsilon_{\mathrm{st}},\epsilon_{\mathrm{op}}) = g_\iota(\epsilon_{\mathrm{st}}) - g_\iota(\epsilon_{\mathrm{op}}) \quad (6)$$

where r_{c} is the cavity radius. The solution phase transition energy is given by

$$E_{\mathrm{sol}} = E_{\mathrm{i}}^{\mathrm{eq}} - E_{\mathrm{f}}^{\mathrm{neq}} \quad (7)$$

D. Cavity Radius. The radius of the solvent cavity containing the solute, r_{c}, is an important parameter that significantly influences the computational results. Although it can be quantified in a number of different ways,[3,32] it is essential to ascertain that the r_{c} value used is also physically reasonable. Use of spherical cavities, of course, makes calculations less complicated. Moreover, for the present study, a spherical cavity seems to fit the M−O_2 complex quite well. For the work reported here, r_{c} was obtained in the following manner: (1) an equilibrium nuclear geometry was calculated for the given configuration/orientation of the solute, (2) the solute center-of-mass was then determined, (3) the distance, *d*, from the center-of-mass to the most distant nucleus was obtained, and (4) the van der Waals radius of that particular distant nucleus was added to *d*.

E. The Wave Function. Molecular oxygen is an open-shell system, and therefore the corresponding complexes are also open-shell systems. This means that it is not advisable to use correlated methods based on a single determinant reference wave function. Instead, we used the multiconfigurational self-consistent field, MCSCF, approach. In the work with the isolated oxygen molecule, the 1s and 2s electrons were considered inactive and the complete active space was given by correlating eight electrons in eight orbitals. We performed the calculations with both the aug-cc-pVDZ and aug-cc-pVQZ basis sets and observed only minor differences in the calculated solvent shifts. For the M−O_2 complexes, however, all calculations were performed with the aug-cc-pVDZ basis set. This basis set is sufficiently large and flexible for describing the physical problem. The calculations were performed with the DALTON program package.[33] We used response theory[34] to calculate frequency-dependent polarizabilities and, when using sufficiently flexible basis sets, this method has been shown to include the continuum contributions in the calculations of the response properties.[35,36]

For all M−O_2 complexes, including those in which M has a comparatively large permanent dipole moment, the M and O_2 interaction energies are weak. This means that the potential surfaces all turn out to be very shallow. In general, the minima of the potential surfaces were found when the distance between M and O_2 was about 3.5−4.0 Å. At this distance, the natural MOs of the complex and their occupation numbers do not deviate significantly from those of the separate molecules. Therefore, we use the symmetry notation of the separated molecules for the MO assignment in the complex. Moreover, since the solvent molecule remains in it's ground state, we use the state assignment of the oxygen molecule for the complex.

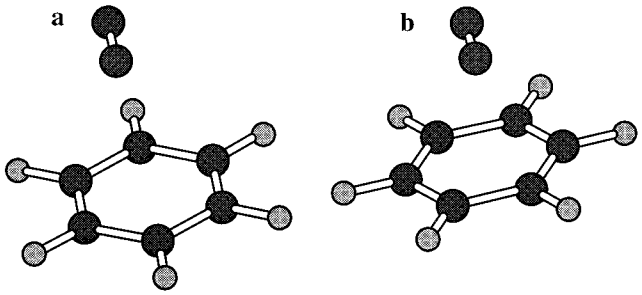

Figure 1. Structures for the C_6H_6−O_2 complex.

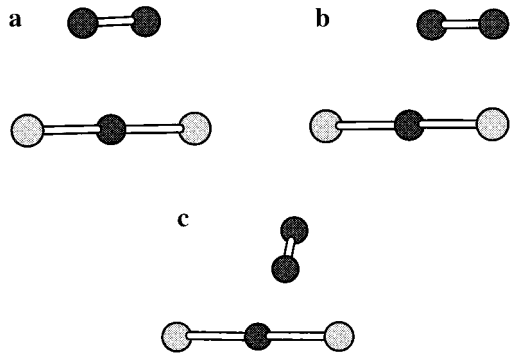

Figure 2. Structures for the CS_2−O_2 complex.

For the benzene−O_2 complex we considered the orientations shown in parts a and b of Figure 1. Both are of C_{2v} symmetry. For the benzene part we chose the full π valence space as the active space for the MCSCF calculations. The oxygen part of the wave function contains a complete active space with $(3\sigma_{\mathrm{g}})$-$(\pi_{\mathrm{u}})(\pi_{\mathrm{g}})(3\sigma_{\mathrm{u}})$ MOs. In the C_{2v} point group, the degenerate π_{u} and π_{g} oxygen orbitals split into orbitals of different symmetry. Thus, we correlate 14 active electrons (6 from benzene and 8 from oxygen) in 12 orbitals (6 from the oxygen part of the wave function). We use the same complete active space, CAS, for the oxygen part of the wave function in the calculations on all the complexes.

The orientations for the M−O_2 complexes containing the other solvent molecules are shown in Figures 2−5. The CAS for these solvents are chosen to be similar in size to that of benzene, and the choice of CAS is motivated by calculations on the isolated solvent molecules.

Results and Discussion

A. Dispersion Interactions: Consideration of a M−O_2 Complex. In Figures 6 and 7, we plot the frequency-dependent polarizabilities, α, for the ground, $X^3\Sigma_g^-$, and excited, $a^1\Delta_g$, states of the two C_6H_6−O_2 complexes. We employ the average value calculated from $\bar{\alpha} = (\alpha_{xx} + \alpha_{yy} + \alpha_{zz})/3$. For each state, the polarizability increases with an increase in the frequency, as expected.[37] However, for small frequencies we observe a slight decrease in the excited-state polarizability for both M−O_2 orientations. Further investigation of the individual polarizability components reveals that this decrease derives from the behavior of α_{xx}, which is the component in the plane of the benzene ring but perpendicular to the oxygen internuclear axis. In the isolated

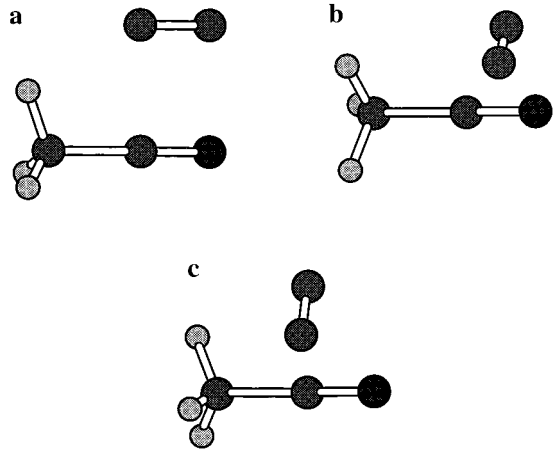

Figure 3. Structures for the CH_3CN-O_2 complex.

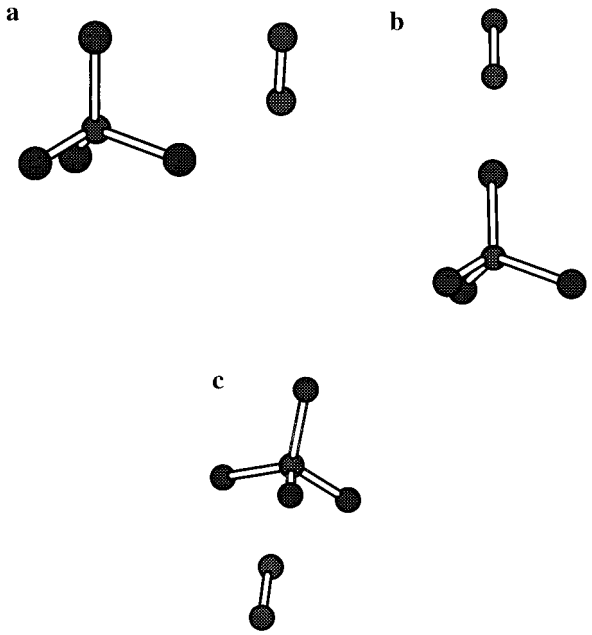

Figure 4. Structures for the CCl_4-O_2 complex.

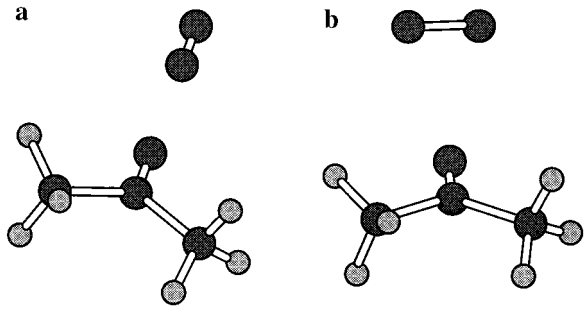

Figure 5. Structures for the $(CH_3)_2CO-O_2$ complex.

oxygen molecule, the $\pi_{g,x}$ and $\pi_{g,y}$ orbitals are degenerate. At the $M-O_2$ interaction distance of ~3.5−4.0 Å, the benzene π system lifts this degeneracy by selectively interacting with the $\pi_{g,y}$ orbital. It is thus possible that the behavior of α_{xx} is simply a consequence of this perturbation-dependent splitting of π_g orbitals and the corresponding decrease in the extent to which the $\pi_{g,x}$ orbital is occupied.

As in our recent work on the isolated oxygen molecule,[13] we find that the polarizabilities for the $a^1\Delta_g$ and $X^3\Sigma_g^-$ states of the complexes are likewise similar in magnitude, and that the excited state polarizability can even be slightly smaller than

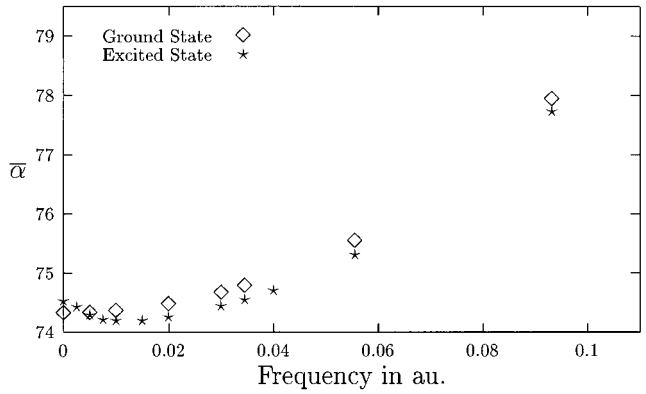

Figure 6. Plots of dynamic average polarizabilities, $\bar{\alpha}$, for the excited and ground states of the benzene$-O_2$ complex shown in Figure 1a. Polarizabilities are given in atomic units.

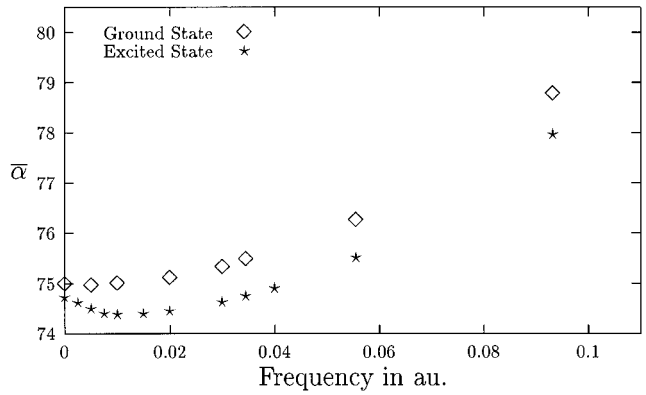

Figure 7. Plots of dynamic average polarizabilities, $\bar{\alpha}$, for the excited and ground states of the benzene$-O_2$ complex shown in Figure 1b. Polarizabilities are given in atomic units.

the ground state polarizability. This means that even though we consider a $M-O_2$ complex, the experimentally observed $a \rightarrow X$ solvent shifts[7,8] cannot be described by simple dispersion interactions such as those from the London formula.

B. Continuum Model. Solvent shifts were calculated using the dielectric continuum model in which electrostatic interaction terms are considered for an isolated oxygen molecule surrounded by solvent. Our data are compared with experimental values in Table 1. We first notice that the calculated solvent shifts are insensitive to a change in basis set, which suggests that the results are reliable. More important, however, is the large deviation from experimental values, which are all consistently smaller than the calculated shifts. This deviation indicates that the comparatively simple continuum model is not sufficient, and that one most likely needs to include a first solvation shell in which short-range $M-O_2$ interactions are considered.

C. Semicontinuum Model: Solvated $M-O_2$ Complexes. Spectral shifts were calculated using the semicontinuum model in which Coulombic and dispersion interaction terms are considered for a solvated $M-O_2$ complex. Our data are compared with experimental values in Table 2. Contrary to the results obtained utilizing the continuum model, we now consistently observe solvent shifts that correlate well with experimental data. Moreover, in this improved model, it appears sufficient to only include a single solvent molecule in the "solvation shell". This is consistent with the notion that the perturbation of oxygen occurs in a 1:1 molecular complex between M and O_2.[6,12,38] Our data thus indicate that it is feasible to perform meaningful high-level ab initio calculations on this system.

TABLE 3: Solvation Energies, *E*, for M−O_2 ($a^1\Delta_g$) and M−O_2 ($X^3\Sigma_g^-$) Complexes as a Function of the Coupling Terms between the Complex and the Outer Solvent

	benzene−oxygen complex[a]			CS_2−oxygen complex[b]		
ι_{max}[c]	$E(a^1\Delta_g)$[d] (cm^{-1})	$E(X^3\Sigma_g^-)$[e] (cm^{-1})	$\Delta\nu_{calc}$ (cm^{-1})	$E(a^1\Delta_g)$[d] (cm^{-1})	$E(X^3\Sigma_g^-)$[e] (cm^{-1})	$\Delta\nu_{calc}$ (cm^{-1})
1	−0.17	−0.02	−0.15	−0.5	−10.5	+10.0
2	−37.3	−54.6	+17.3	−5.5	−16.2	+10.7
3	−94.5	−82.1	−12.4	−15.9	−18.1	+2.2
4	−103.0	−82.0	−21.0	−27.5	−20.1	−7.4
5	−103.6	−87.0	−16.6	−38.3	−21.8	−16.5
6	−118.8	−91.3	−27.5	−51.7	−23.4	−28.3
7	−124.9	−93.3	−31.6	−59.6	−23.7	−35.9
8	−126.2	−93.6	−32.6	−65.8	−24.0	−41.8
9	−127.7	−94.1	−33.6	−69.9	−24.5	−45.4
10	−128.6	−94.6	−34.0	−72.5	−24.8	−47.7

[a] The data shown are for the M−O_2 orientation shown in Figure 1b. [b] The data shown are for the M−O_2 orientation shown in Figure 2b. [c] Number of terms in the multipole expansion that are used to calculate the solvation energy (e.g., $\iota_{max} = 1$, dipolar term only; $\iota_{max} = 2$, quadrupolar and dipolar terms together; $\iota_{max} = 3$, octapolar, quadrupolar, and dipolar terms together; etc.). [d] $E(a^1\Delta_g) = E_i^{eq} - E_i$ (gas). [e] $E(X^3\Sigma_g^-) = E_f^{neq} - E_f$ (gas).

As can be seen in Table 2, the calculated energies depend strongly on the orientations of M and O_2 in the complex. This is to be expected for such a perturbation-sensitive transition, and it demonstrates the need to consider multiple orientations of M and O_2. The data in Table 2 also indicate that, to obtain a more accurate average of calculated spectral shifts, one should ideally consider a much larger sampling of M and O_2 orientations. This could be accomplished by deriving a M−O_2 interaction potential and performing a molecular dynamic simulation.[39,40] Moreover, we find that the solvation energies of the M−O_2($a^1\Delta_g$) and M−O_2($X^3\Sigma_g^-$) complexes depend principally on the quadrupolar and higher order coupling terms between the complex and the outer solvent, and only slightly on the dipolar coupling term (Table 3). This demonstrates that one must not only consider the short-range interactions found in the M−O_2 complex but that coupling between the complex and the outer solvent is a critical component in defining the spectral shift.

Conclusion

We have presented a model that appears to accurately represent the effect of solvent on a → X spectral shifts in molecular oxygen. The key components of this model include (1) a molecular complex between one solvent molecule, M, and O_2 that accounts for short-range interactions, (2) solvation of the M−O_2 complex in an outer solvent represented as a dielectric continuum that accounts for long-range Coulombic interactions, and (3) consideration of equilibrium as well as nonequilibrium solvation conditions. Moreover, the a → X spectral shifts cannot be described solely by dispersion interactions obtained from the London formula.

Acknowledgment. This work was supported by grants from Aarhus University, the Danish Natural Science Research Council (9601705), and the Natural Science Council Center for Molecular Dynamics and Laser Chemistry.

References and Notes

(1) Weldon, D.; Ogilby, P. R. *J. Am. Chem. Soc.* **1998**, *120*, 12978−12979.
(2) Weldon, D.; Wang, B.; Poulsen, T. D.; Mikkelsen, K. V.; Ogilby, P. R. *J. Phys. Chem. A* **1998**, *102*, 1498−1500.
(3) Poulsen, T. D.; Ogilby, P. R.; Mikkelsen, K. V. *J. Phys. Chem. A* **1998**, *102*, 9829−9832.
(4) Scurlock, R. D.; Nonell, S.; Braslavsky, S. E.; Ogilby, P. R. *J. Phys. Chem.* **1995**, *99*, 3521−3526.
(5) Schmidt, R.; Bodesheim, M. *J. Phys. Chem.* **1995**, *99*, 15919−15924.
(6) Schmidt, R. *J. Phys. Chem.* **1996**, *100*, 8049−8052.
(7) Macpherson, A. N.; Truscott, T. G.; Turner, P. H. *J. Chem. Soc., Faraday Trans.* **1994**, *90*, 1065−1072.
(8) Wessels, J. M.; Rodgers, M. A. J. *J. Phys. Chem.* **1995**, *99*, 17586−17592.
(9) Minaev, B. F.; Ågren, H. *J. Chem. Soc., Faraday Trans.* **1997**, *93*, 2231−2239.
(10) Ogilby, P. R. *Acc. Chem. Res.*, in press.
(11) Herzberg, G. *Molecular Spectra and Molecular Structure. I. Spectra of Diatomic Molecules*; 2nd ed.; Van Nostrand Reinhold: New York, 1950.
(12) Lin, S. H.; Lewis, J.; Moore, T. A. *J. Photochem. Photobiol. A: Chem.* **1991**, *56*, 25−34.
(13) Poulsen, T. D.; Ogilby, P. R.; Mikkelsen, K. V. *J. Phys. Chem. A* **1998**, *102*, 8970−8973.
(14) Mikkelsen, K. V.; Dalgaard, E.; Swanstrøm, P. *J. Phys. Chem.* **1987**, *91*, 3081−3092.
(15) Mikkelsen, K. V.; Ågren, H.; Jensen, H. J. A.; Helgaker, T. *J. Chem. Phys.* **1988**, *89*, 3086−3095.
(16) Mikkelsen, K. V.; Cesar, A.; Ågren, H.; Jensen, H. J. A. *J. Chem. Phys.* **1995**, *103*, 9010−9023.
(17) *Handbook of Chemistry and Physics*, 74th ed.; Lide, D. R., Ed.; CRC Press: Boca Raton, 1994.
(18) Vahtras, O.; Ågren, H.; Jørgensen, P.; Jensen, H. J. A.; Helgaker, T.; Olsen, J. *J. Chem. Phys.* **1992**, *97*, 9178−9187.
(19) Mikkelsen, K. V.; Jørgensen, P.; Jensen, H. J. A. *J. Chem. Phys.* **1994**, *100*, 6597−6607.
(20) Mikkelsen, K. V.; Sylvester-Hvid, K. O. *J. Phys. Chem.* **1996**, *100*, 9116−9126.
(21) Mikkelsen, K. V. *Z. Phys. Chem.* **1991**, *170*, 129−142.
(22) Marcus, R. A. *J. Phys. Chem.* **1992**, *96*, 1753−1757.
(23) Young, R. H. *J. Chem. Phys.* **1992**, *97*, 8261−8275.
(24) Kim, H. J.; Bianco, R.; Gertner, B. J.; Hynes, J. T. *J. Phys. Chem.* **1993**, *97*, 1723−1728.
(25) Marcus, R. A. *J. Chem. Phys.* **1956**, *24*, 979−989.
(26) Jortner, J. *Mol. Phys.* **1962**, *5*, 257−270.
(27) Felderhof, B. U. *J. Chem. Phys.* **1977**, *67*, 493−500.
(28) Lee, S.; Hynes, J. T. *J. Chem. Phys.* **1988**, *88*, 6853−6862.
(29) Kim, H. J.; Hynes, J. T. *J. Chem. Phys.* **1990**, *93*, 5194−5210.
(30) McRae, E. G. *J. Phys. Chem.* **1957**, *61*, 562−572.
(31) Bayliss, N. S.; McRae, E. G. *J. Phys. Chem.* **1954**, *58*, 1002−1006.
(32) Luo, Y.; Ågren, H.; Mikkelsen, K. V. *Chem. Phys. Lett.* **1997**, *275*, 145−150.
(33) Helgaker, T.; Jensen, H. J. A.; Jørgensen, P.; Olsen, J.; Ruud, K.; Ågren, H.; Andersen, T.; Bak, K. L.; Bakken, V.; Christiansen, O.; Dahle, P.; Dalskov, E. K.; Enevoldsen, T.; Fernandez, B.; Heiberg, H.; Hettema, H.; Jonsson, D.; Kirpekar, S.; Kobayashi, R.; Koch, H.; Mikkelsen, K. V.; Norman, P.; Packer, M. J.; Saue, T.; Taylor, P. R.; Vahtras, O. *Dalton*, an ab initio electronic structure program, release 1.0, 1997. See http://www.kjemi.uio.no/software/dalton/dalton.html.
(34) Olsen, J.; Jørgensen, P. *J. Chem. Phys.* **1985**, *82*, 3235−3264.
(35) Olsen, J.; Jørgensen, P. In *Modern Electronic Structure Theory*; Yarkony, D. R., Ed.; Advanced Series in Physical Chemistry; World Scientific: Singapore, 1995; Part II, pp 857−990.
(36) Carravetta, V.; Ågren, H.; Jensen, H. J. A.; Jørgensen, P.; Olsen, J. *J. Phys. B* **1989**, *22*, 2133−2140.
(37) Bloembergen, N. *Nonlinear Optics*; Benjamin: Reading, 1965.
(38) Scurlock, R. D.; Ogilby, P. R. *J. Phys. Chem.* **1987**, *91*, 4599−4602.
(39) Nymand, T. M.; Åstrand, P.-O.; Mikkelsen, K. V. *J. Phys. Chem. B* **1997**, *101*, 4105−4110.
(40) Sylvester-Hvid, K. O.; Nymand, T. M.; Åstrand, P.-O.; Mikkelsen, K. V. *J. Phys. Chem. A.*, in press.